Appl. Phys. A 79, 1635–1641 (2004)
DOI: 10.1007/s00339-004-2676-0

Applied Physics A
Materials Science & Processing

C.H. CROUCH[1,2,*]
J.E. CAREY[2]
M. SHEN[2]
E. MAZUR[1,2,✉]
F.Y. GÉNIN[3]

Infrared absorption by sulfur-doped silicon formed by femtosecond laser irradiation

[1] Department of Physics, Harvard University, 9 Oxford St., Cambridge, MA 02138, UK
[2] Division of Engineering and Applied Sciences, Harvard University, 9 Oxford St., Cambridge, MA 02138, UK
[3] Lawrence Livermore National Laboratory, Livermore, CA USA

Received: 13 August 2003/Accepted: 4 February 2004
Published online: 23 June 2004 •

ABSTRACT We microstructured silicon surfaces with femtosecond laser irradiation in the presence of SF_6. These surfaces display strong absorption of infrared radiation at energies below the band gap of crystalline silicon. We report the dependence of this below-band gap absorption on microstructuring conditions (laser fluence, number of laser pulses, and background pressure of SF_6) along with structural and chemical characterization of the material. Significant amounts of sulfur are incorporated into the silicon over a wide range of microstructuring conditions; the sulfur is embedded in a disordered nanocrystalline layer less than 1 μm thick that covers the microstructures. The most likely mechanism for the below-band gap absorption is the formation of a band of sulfur impurity states overlapping the silicon band edge, reducing the band gap from 1.1 eV to approximately 0.4 eV.

PACS 78.68.+m; 81.15.Fg; 81.40.Tv; 81.65.Cf; 85.60.Gz

1 Introduction

Silicon is widely used for solar cells and photodetectors, but the band gap of crystalline silicon renders it transparent to wavelengths longer than 1.16 μm; amorphous silicon and microcrystalline silicon have band gaps similar to crystalline silicon. Silicon is, therefore, not used to absorb or detect light at wavelengths longer than 1.1 μm. Near-infrared detectors for wavelengths longer than 1.1 μm are widely used for both telecommunications and scientific instrumentation. Consequently, a silicon-based near-infrared detector that can be integrated with other electronics through standard silicon processing has many applications.

We previously reported that silicon surfaces microstructured in the presence of SF_6 with high-intensity femtosecond laser pulses have near-unity absorption from the near-ultraviolet (250 nm) to the near-infrared (2.5 μm) [1, 2]. We recently found that microstructuring in H_2S [3] or in the presence of elemental sulfur has the same effect, as does microstructuring with excimer laser pulses in the presence of SF_6 [4, 5]; microstructuring in gases that do not contain sulfur does not produce comparable below-band gap absorption [3, 6]. Silicon surfaces microstructured in SF_6 also produce significant photocurrent from 1.31 or 1.55 μm illumination [7].

Here we report the effects of processing conditions and thermal annealing on the below-band gap absorption, chemical composition, and lattice structure of these microstructured silicon surfaces. We observe below-band gap absorption in samples produced under a wide range of conditions; the maximum wavelength of strong below-band gap absorption is 3.5 μm. We attribute the absorption to sulfur impurities in a nanocrystalline layer covering the microstructures.

2 Experimental methods

The samples are microstructured by irradiating a silicon (111) wafer (n-Si(111), 260 μm thick, with resistivity $\varrho = 8$–$12\ \Omega$ m) with a train of 800-nm, 100-fs laser pulses in the presence of SF_6 [2]. The samples discussed in this paper were all made on the same substrate silicon; we previously found that the doping, resistivity, and crystal plane of the initial substrate do not affect the optical properties. Irradiation creates a quasi-ordered array of microstructures on the surface of the sample. The microstructures form only in the region illuminated by the laser. We microstructured areas up to 10 mm × 10 mm by scanning the laser beam across the sample; the laser fluence [8] and average number of pulses delivered to each region of the sample determined the shape and depth of the microstructures. The number of pulses was set by the scan speed, the size of the laser spot on the sample surface, and the repetition rate of the laser [9].

We determined the absorptance (A) of the microstructured surfaces by measuring the total hemispherical (specular and diffuse) reflectance (R) and transmittance (T) with a UV-VIS spectrophotometer equipped with an integrating sphere detector; we then calculated the absorptance $A = 1–R–T$. We measured transmittance at longer wavelengths with a Fourier transform infrared spectrophotometer.

3 Experimental results

Figure 1 shows the microstructures formed by laser irradiation under our standard conditions of 500 laser pulses, 8 kJ/m^2, and 0.67 bar SF_6. These conditions produce sharp

✉ Fax: +1-240/255-4622, E-mail: mazur@physics.harvard.edu
**Present address*: Dept. of Physics & Astronomy, Swarthmore College, Swarthmore, PA 19081

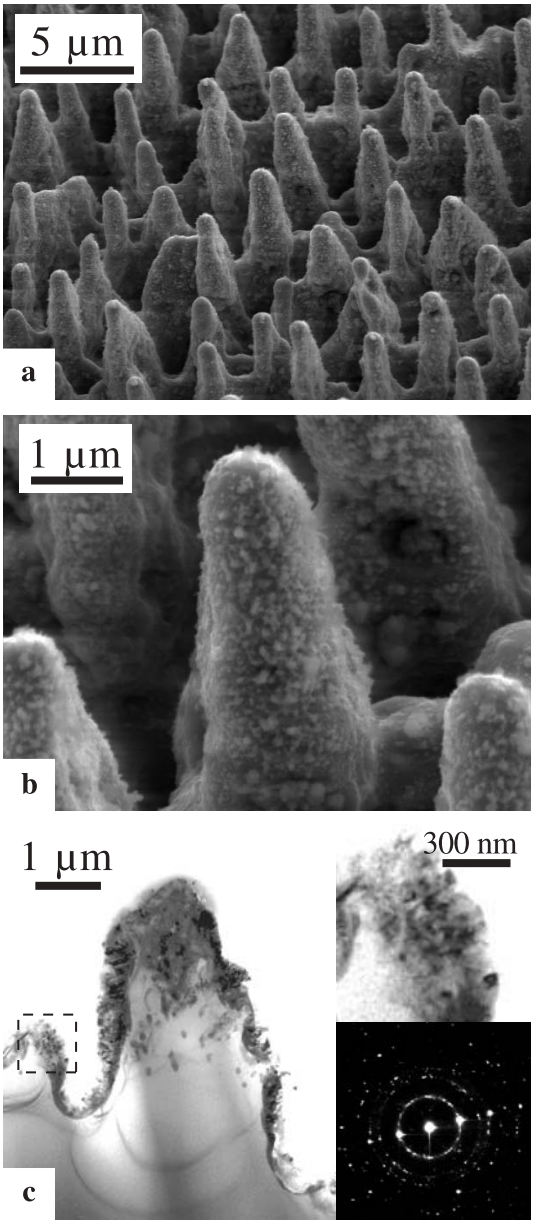

FIGURE 1 **a**,**b** Scanning electron micrographs of laser-microstructured silicon surface formed in SF_6 under "standard" conditions for this paper (laser pulse duration: 100 fs; 500 laser pulses; laser fluence: 8 kJ/m^2; SF_6 pressure: 0.67 bar). The sample is viewed at 45° to the normal. **c** Bright-field transmission electron micrograph of cross-section through a row of microstructures. *Insets*: (*upper*) high-magnification view of the disordered region at the tip of the spike (indicated on main image with *dashed square*) and (*lower*) selected area electron diffraction pattern obtained from the disordered region

conical microstructures about 8 μm tall and 1 μm across at the tip, separated by 3–4 μm (Fig. 1a), and covered with nanoscale particles (Fig. 1b). As can be seen in the bright-field transmission electron micrograph of a cross-section through one of the microstructures (Fig. 1c), the microstructures consist of a crystalline silicon core covered with a layer of disordered material less than 1 μm thick. The surface layer contains silicon nanocrystals (∼ 10–50 nm in diameter), pores, and impurities. Selected-area electron diffraction (inset) indicates that the surface layer has a crystalline order. Energy dispersive X-ray emission spectroscopy indicates a sulfur concentration of roughly 1% in this layer; there is no detectable sulfur in the crystalline core.

Figure 2 shows scanning electron micrographs of the microstructures formed with an increasing number of laser pulses (a–c), laser fluence (d–f), and the background pressure of SF_6 (g–i). All of these samples were made by varying just one processing condition relative to the standard conditions of Fig. 1. At fewer than 10 laser pulses or less than 4 kJ/m^2 fluence, we observe ridges parallel to the laser polarization rather than conical microstructures. Increasing the number of laser pulses or laser fluence produces conical microstructures that are shorter and blunter than those obtained under the standard conditions. For SF_6 pressures between 27 mbar and 400 mbar, ridges form; at lower pressures, larger, blunt structures form.

Figure 3 shows that the absorptance at 1550 nm increases strongly with the number of pulses delivered to the sample, up to 20 pulses; additional pulses have little effect. The inset shows that the absorptance increases over the entire wavelength range as the number of laser pulses increases. For unstructured (crystalline) silicon, the absorptance drops sharply around 1.16 μm, corresponding to the band gap of silicon, and is very low for longer wavelengths. For the microstructured samples, the absorptance is essentially constant between 1.2 and 2.5 μm, with its value increasing with the number of pulses.

Figure 4 shows that the absorptance at 1550 nm increases strongly with fluence for fluences up to about 5 kJ/m^2 and increases more slowly for higher fluences. Surfaces made with 4 kJ/m^2 or more display constant absorptance vs. wavelength at below-band gap wavelengths; at lower fluences, the absorptance decreases gradually with increasing wavelength. With 500 laser pulses, fluences below 2.5 kJ/m^2 do not produce uniform microstructuring of the surface (fluence less than 2.0 kJ/m^2 neither alters the surface nor affects the optical properties).

Figure 5 shows that the absorptance also increases with increasing SF_6 pressure, and the greatest rate of increase is observed at low pressures. Above 27 mbar, the below-band gap absorptance does not vary with wavelength, while at lower pressure, it decreases with increasing wavelength. For samples made in vacuum, the gradual decrease of absorptance for wavelengths longer than 1.2 μm is consistent with the presence of band tails of Urbach states due to a high density of defects [10].

Figure 6 shows the effects of annealing for 30 minutes in flowing Ar on the absorptance of samples made under standard conditions. Annealing at temperatures below 575 K has little effect on the absorptance. Annealing between 575 K and 875 K does not affect absorptance above the band gap, but lowers the below-band gap absorptance; the higher the temperature, the greater the decrease in absorptance. Raising the annealing temperature above 875 K does not produce any additional change. As shown in Fig. 7, annealing has no visible effect on the shape of either the microstructures or the surface nanoparticles.

To determine the extent of the below-band gap absorptance, we measured specular infrared transmittance at wavelengths longer than 2.5 μm. For a standard sample (8 kJ/m^2, 500 pulses, 0.67 bar SF_6), the transmittance is only a few percent at 2.5 μm but begins to rise at approximately 3.5 μm,

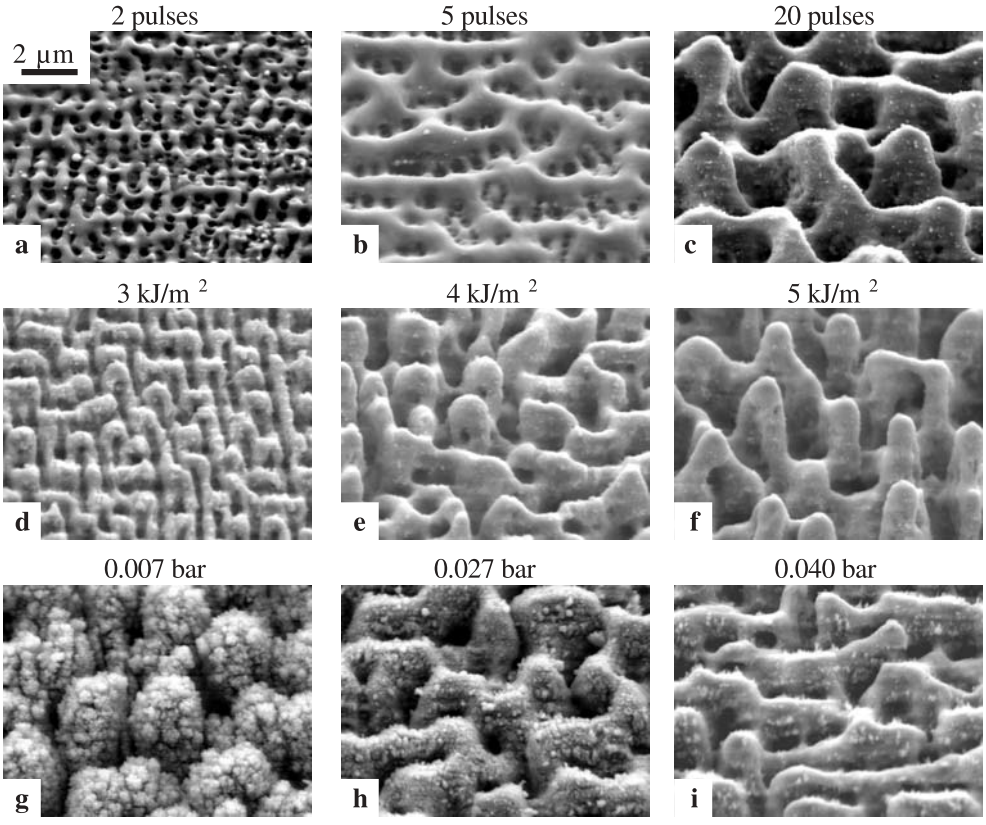

FIGURE 2 Scanning electron micrographs of laser-microstructured silicon surfaces formed in SF_6 with **a** 2, **b** 5, and **c** 20 laser pulses (fluence: 8 kJ/m^2; SF_6 pressure: 0.67 bar); with laser fluence **d** 3, **e** 4, and **f** 5 kJ/m^2 (500 pulses, 0.67 bar SF_6); with SF_6 pressure **g** 7 mbar, **h** 27 mbar, and **i** 400 mbar (500 pulses, 8 kJ/m^2). Samples are viewed at 45° to the normal

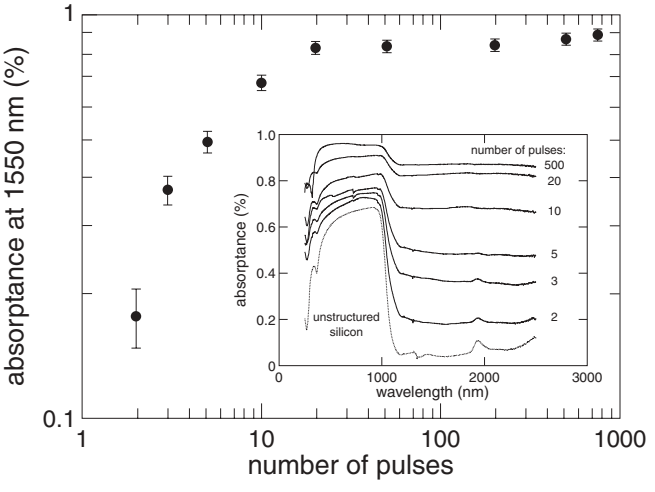

FIGURE 3 Dependence of the absorptance at 1550 nm of microstructured silicon surfaces on the number of laser pulses used in microstructuring. All samples were made with 8 kJ/m^2 laser fluence and 0.67 bar SF_6 pressure. Inset: Wavelength dependence of absorptance for a subset of the samples shown in Fig. 3 and for the unstructured silicon substrate

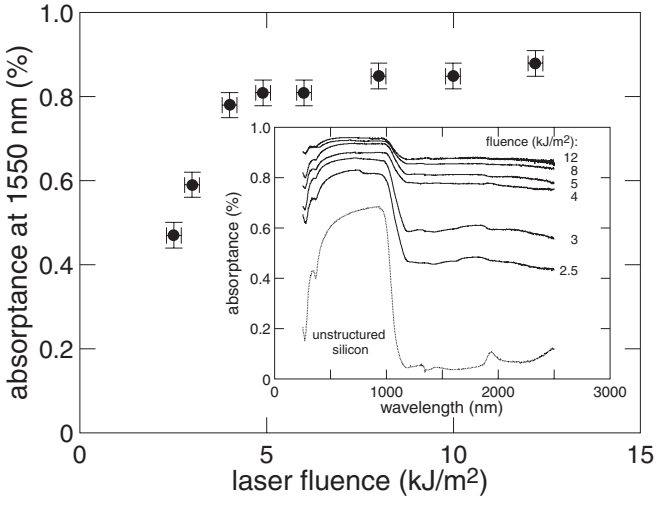

FIGURE 4 Dependence of the absorptance at 1550 nm of microstructured silicon surfaces on the laser fluence used in microstructuring. All samples were made with 500 laser pulses and 0.67 bar SF_6 pressure. *Inset*: Wavelength dependence of the absorptance for a subset of the samples shown in Fig. 4 and for the unstructured silicon substrate

and reaches 50% at roughly 6 μm. Because this measurement was not made with an integrating sphere, scattering reduces the transmittance; 3.5 μm is therefore an upper bound on the wavelength at which the below-band gap absorptance begins to decrease.

To determine the effect of the microstructuring parameters on lattice structure and chemical composition of the microstructures, we performed Rutherford backscattering spectroscopy (RBS) on selected samples. We measured the backscattering spectrum from 2.0 MeV alpha particles with an annular solid state detector. To determine the chemical composition of the microstructured material, we compared the measured RBS spectra to simulated spectra [11] from planar material. The observable sulfur signal measures only the average sulfur concentration in the uppermost 100 nm of the surface; the RBS signal from deeper sulfur is masked by the silicon signal. Transmission electron microscopy indicates that the uppermost few hundred nanometers of the structures is modified, with crystalline silicon beneath (Fig. 1c), and energy dispersive X-ray emission spectroscopy indicates that

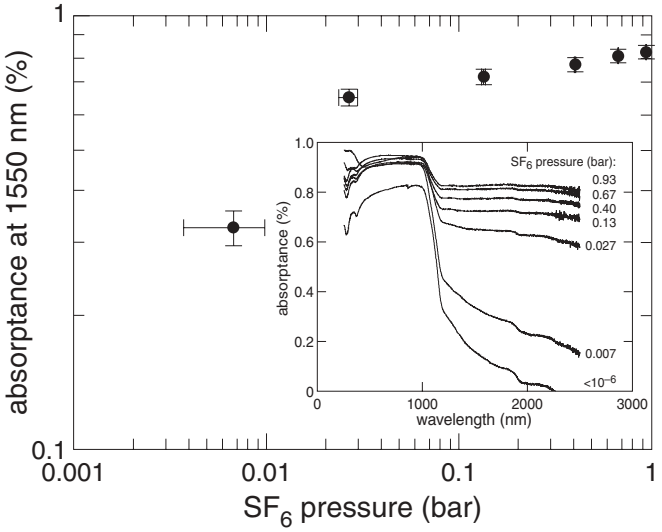

FIGURE 5 Dependence of the absorptance at 1550 nm of microstructured silicon surfaces on the pressure of SF_6 used in microstructuring. All samples were made with 500 laser pulses and 8 kJ/m^2 laser fluence. *Inset*: Wavelength dependence of absorptance for a subset of the samples shown in Fig. 5 and one made in vacuum (base pressure less than 10^{-6} bar)

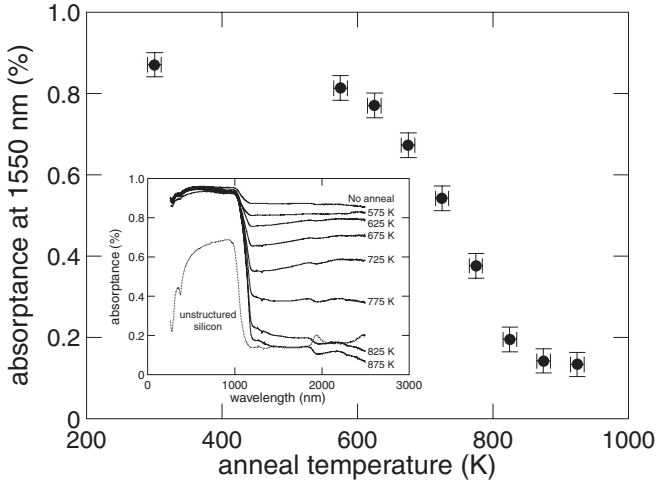

FIGURE 6 Effect of annealing temperature on absorptance at 1550 nm of microstructured silicon surfaces. The data point at room temperature (300 K) corresponds to a sample that was not annealed. All samples were made with 500 laser pulses and 8 kJ/m^2 laser fluence in 0.67 bar SF_6, and were annealed for 30 minutes. *Inset*: Wavelength dependence of absorptance for the samples shown in Fig. 6 and for the unstructured silicon substrate

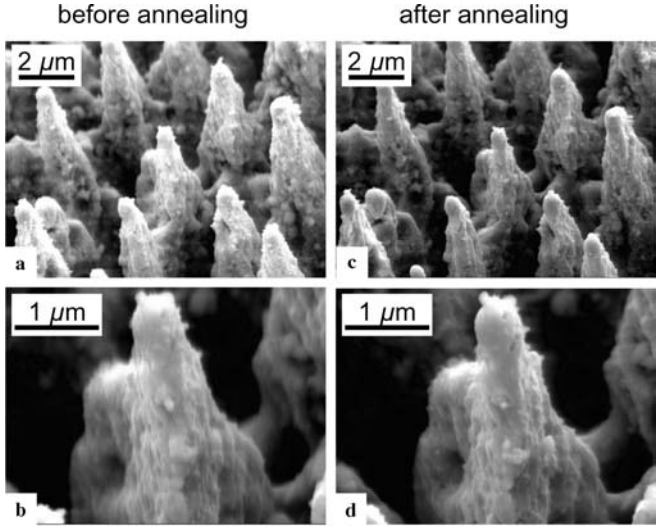

FIGURE 7 Microstructured silicon **a**,**b** before annealing and **c**,**d** after annealing at 800 K for 3 h. The same region of the sample is shown in all four panels

Average laser fluence (kJ/m^2)	Number of pulses	Annealing temperature (30 min)	Sulfur concentration ±0.1 at. %	Absorptance at 1550 nm
2.5	500	–	0.3	0.47
3.0	500	–	0.3	0.59
4.0	500	–	0.4	0.78
4.9	500	–	0.6	0.81
8.0	500	–	0.7	0.85
10.0	500	–	0.7	0.85
8.0	2	–	0.2	0.18
8.0	3	–	0.4	0.37
8.0	5	–	0.4	0.48
8.0	10	–	0.5	0.68
8.0	20	–	0.6	0.83
8.0	50	–	0.6	0.84
8.0	500	–	0.7	0.87
8.0	500	875 K	0.5	0.14
8.0	500	725 K	0.5	0.54

TABLE 1 Sulfur concentration in samples determined by Rutherford backscattering spectroscopy

the sulfur is in the modified layer. Consequently, to determine sulfur concentrations, we simulate just the modified layer.

The RBS spectra indicate that the modified surface layer consists of oxidized silicon with fluorine and sulfur impurities. Neither the oxide nor the fluorine contributes to the optical properties; etching the samples in 5% HF for 4 min removes the fluorine and the oxide without changing either the sulfur concentration or the optical properties. To simplify simulation of the spectra, we therefore measured RBS spectra on samples etched in HF.

Table 1 shows that the concentration of sulfur follows a trend similar to the below-band gap absorptance with processing conditions. The amount of sulfur increases from roughly 0.2% for the sample made with two pulses to roughly 0.7% for the sample made with 50 pulses. Additional pulses have no effect; the sample made with 500 pulses also has 0.7% sulfur. Likewise, the sulfur content increases from 0.4% for the sample made with 2.5 kJ/m^2 to 0.7% for the sample made with 8 kJ/m^2; the sample made with 10 kJ/m^2 also has 0.7% sulfur.

Sulfur concentrations in the annealed samples, however, do not mirror the below-band gap absorptance. Upon annealing a standard sample at either 725 K or 875 K for 30 min, the sulfur content in both cases decreases by only 40%, while the infrared absorptance decreases by almost an order of magnitude. The concentration of sulfur in the annealed samples is comparable to that of the sample made with 4 kJ/m^2 and 500 pulses, or the sample made with ten pulses and 8 kJ/m^2; for these samples, the infrared absorptance is only 20% less than that of a standard sample [12].

Finally, we performed bright-field transmission electron microscopy (TEM) on cross-sections prepared from a sample made with 10 laser pulses, a sample made with a laser

fluence of 4 kJ/m^2, and an annealed standard sample. These micrographs are shown in Fig. 8. We find that the samples made with 10 pulses (Fig. 8a) and 4 kJ/m^2 (Fig. 8b) show a disordered surface layer that is similar to that of the sample made under standard conditions (Fig. 1c), although the microstructures themselves are smaller than the microstructures made under standard conditions. The annealed sample (Fig. 8c) also has a disordered surface layer similar to the non-annealed standard sample of Fig. 1c. Selected area diffraction indicates that for all three samples, the surface layer (insets to Fig. 8) has significant crystalline order, and the core is crystalline. The diffraction rings are sharper for the annealed sample (Fig. 8c) than for the others, which most likely indicates that annealing increases the crystallinity of the sample somewhat, as would be expected. Other factors such as the different crystal plane of the specimen could also sharpen the diffraction pattern.

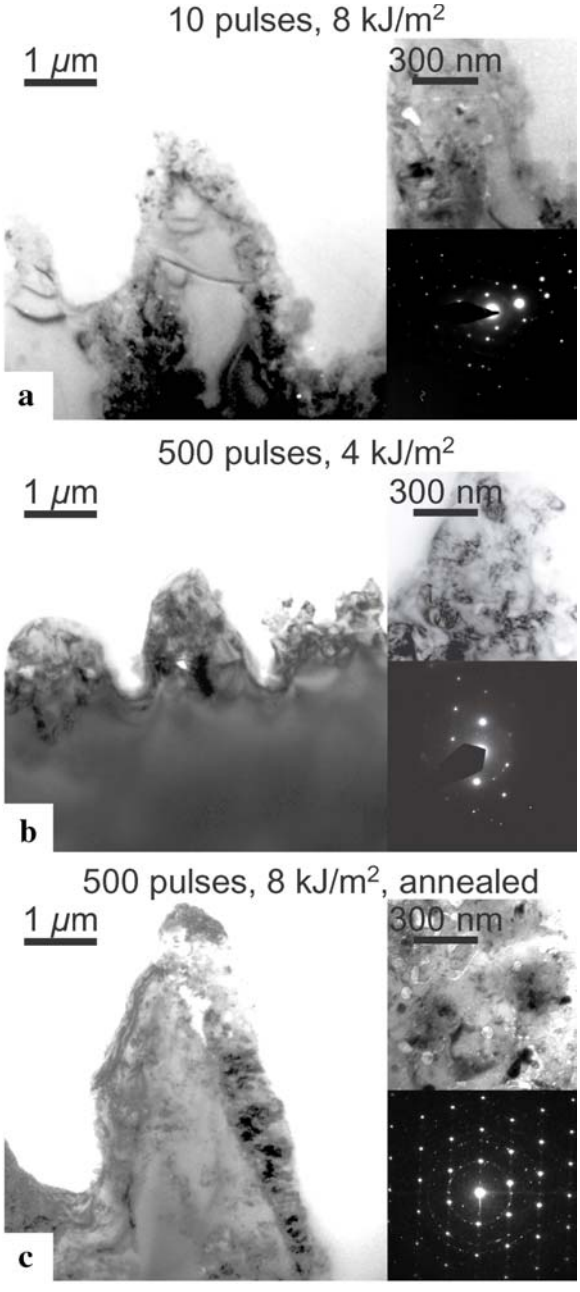

FIGURE 8 Bright-field transmission electron micrographs of cross-sections of microstructures formed with **a** 10 laser pulses, laser fluence 8 kJ/m^2; **b** 500 laser pulses, laser fluence 4 kJ/m^2; and **c** 500 laser pulses, laser fluence 8 kJ/m^2, and annealed at 875 K for 30 minutes. All three samples were made in 0.67 bar SF_6. *Insets*: (*upper*) high-magnification view of the disordered region at the tip of the spike and (*lower*) selected area electron diffraction pattern obtained from the disordered region

4 Discussion

Surfaces laser-microstructured in SF_6 using a wide range of processing conditions exhibit strong, featureless below-band gap absorptance from 1.2 to at least 2.5 μm. The samples also display very high visible absorptance, as reported previously; as the visible absorptance is not affected by annealing, we attribute it to amplification of the intrinsic visible absorptance of ordinary silicon by multiple reflections [2]. The transmittance at longer infrared wavelengths rises at roughly 3.5 μm, indicating that the absorptance decreases in this wavelength range. These optical properties suggest an altered band structure in which the band gap is reduced to roughly 0.4 eV. Further evidence for this altered band structure comes from our recent finding that the microstructured material has a diodic I–V characteristic and high photoresponse to wavelengths longer than 1.1 μm, indicating that the band gap of the surface layer is different from that of the substrate [7].

We attribute this altered band structure to the formation of an impurity band due to the presence of high concentrations of sulfur in the nanocrystalline layer at the surface of the sample. We established previously that sulfur is essential to the below-band gap absorptance; surfaces microstructured in the presence of sulfur or sulfur-containing gases show strong below-band gap absorptance, while surfaces microstructured in environments that do not contain sulfur show absorptance that resembles that of surfaces structured in vacuum [3, 6]. At low concentrations, sulfur impurities introduce states into the band gap of crystalline silicon [13, 14]. Bands of impurity states can form at concentrations as low as 10^{16} /cm^3 [15], so at the sulfur concentrations we observe, it is plausible that a sulfur impurity band forms.

As described in the previous section, we find significant concentrations of sulfur even in samples processed with very few laser pulses or with laser fluences near the threshold for plasma formation, and such samples display significant below-band gap absorptance. In samples that have not been annealed, the sulfur concentration observed by RBS follows a trend similar to the below-band gap absorptance.

Annealing causes the below-band gap absorptance to decrease in a manner that does not mirror the sulfur concentration. For example, samples annealed at 725 K and at 875 K have the same sulfur concentration, but the absorptance at 1550 nm of the sample annealed at 725 K is five times that of the sample annealed at 875 K. The observed sulfur concentration in the sample annealed at 875 K is the same as that from the 10-pulse or 4-kJ/m^2 samples, but the 10-pulse and 4-kJ/m^2 samples display 80% of the below-band gap absorptance of a standard sample, while the below-band gap absorptance of the sample annealed at 875 K is reduced to essentially the same value as the original substrate silicon. The

decrease in the observed sulfur concentration upon annealing most likely reflects sulfur diffusing deeper into the sample than can be observed by RBS [16].

The annealing results indicate that absorption is not determined by sulfur concentration alone. The most likely explanation of the below-band gap absorption is that laser microstructuring incorporates the sulfur impurities into the silicon matrix in optically active states, and annealing causes bond rearrangement within the silicon matrix that renders the sulfur impurities optically inactive. (Complete recrystallization of the material is not necessary to eliminate the below-band gap absorption; the annealed material is still significantly disordered [17].) It is also possible that optically inactive precipitates or sulfur-silicon complexes form upon annealing.

While we cannot identify specific optically active sulfur states, we do have some information about them. The TEM images of Figs. 1 and 8 indicate that samples made over a wide range of conditions are covered with a layer of nanocrystalline material containing the sulfur impurities. It is known that after ion implantation of sulfur into silicon, the sulfur impurities form complexes with the implantation-induced damage [18]. After laser microstructuring, it is therefore likely that the sulfur is present in close proximity to defects rather than in the nanocrystalline grains. It is also possible that amorphous-like material is present between the nanocrystalline grains. Keblinski et al. [19] found that the structure of the intergranular phase in nanocrystalline silicon is remarkably similar to that of bulk amorphous silicon. The presence of either defects or amorphous material is likely to provide a wide variety of electronic environments for the sulfur impurities, producing a band of impurity states.

Further work is required to determine the mechanism by which sulfur is incorporated into the surface layer. However, the results presented here provide some clues. The sulfur concentrations in our structures exceed the solid solubility of sulfur in silicon [20] by many orders of magnitude, indicating that sulfur is incorporated through a highly nonequilibrium process. The fact that the sulfur content reaches its maximum value with just 20 pulses, and that the surface layer formed with just 10 pulses is similar in both thickness and structure to that formed with 500 pulses, suggests that the surface layer may re-form with each laser pulse once the pattern of microstructures is established. The increase of sulfur with increasing laser fluence indicates that more sulfur is incorporated when more energy is deposited in the surface. This result would be consistent with sulfur being incorporated into a melted layer formed on the surface of the microstructures after equilibration of the electrons with the lattice; such a layer is expected to form [21] because the laser fluences used for these samples are near or not far above the ablation threshold of approximately 3 kJ/m^2 [22].

Silicon can be doped by melting the surface with excimer laser pulses in the presence of a gas containing the desired dopants [23]. The dopants are incorporated into the melt and the rapid solidification that follows laser melting can produce highly supersaturated solid solutions [24]. We recently found that microstructuring with excimer laser pulses [5] also produces strong below-band gap absorptance. Our femtosecond laser microstructuring process may incorporate sulfur in a similar fashion.

5 Conclusions

We report here the dependence of the below-band gap absorptance of laser-structured silicon on the laser conditions used to structure the surface and on the sulfur content of the microstructured surfaces. Our observations suggest an altered band structure in a layer of sulfur-doped nanocrystalline silicon covering the microstructures; the band gap is reduced to roughly 0.4 eV by the formation of a sulfur impurity band. The sulfur may be present in regions of amorphous or highly disordered silicon that fill spaces between submicrometer-size crystalline grains. The dependence of the optical properties on annealing temperature is consistent with sulfur-doped amorphous silicon.

The altered surface layer forms over a wide range of processing conditions; consequently, different conditions can be designed for different applications. For example, for field emitters, high aspect ratio, sharp conical structures can be formed with large numbers of pulses and high fluence; for detectors or other devices fabricated on a heterostructured substrate, lower fluence or fewer pulses can be used to form shallower microstructures, in order not to disrupt the underlying heterostructure.

ACKNOWLEDGEMENTS We thank Dr. J. Chervinsky, J. Harper, E. Hoke, J. Sage, M. Sheehy, and D. Wolfe for experimental assistance, and Prof. M.J. Aziz, Prof. C. Friend, Prof. E. Kaxiras, Prof. J. Leonard, Prof. W. Paul, and Prof. F. Spaepen for helpful discussions. Work at Harvard was supported by the Harvard University MRSEC (NSF/DMR-98-09363), the Department of Energy (DOE DE FC36 01GO11053), and the Army Research Office (DAAD19-99-1-0009). Work at LLNL was performed under the auspices of the U. S. Department of Energy by the University of California, Lawrence Livermore National Laboratory under Contract No. W-7405-Eng-48.

REFERENCES

1 T.-H. Her, R.J. Finlay, C. Wu, S. Deliwala, E. Mazur: Appl. Phys. Lett. **73**, 1673 (1998)
2 C. Wu, C.H. Crouch, L. Zhao, J.E. Carey, R. Younkin, J.A. Levinson, E. Mazur, R.M. Farrell, P. Gothoskar, A. Karger: Appl. Phys. Lett. **78**, 1850 (2001)
3 M. Sheehy, L. Winston, J.E. Carey, E. Mazur, C.M. Friend: unpublished results
4 A.J. Pedraza, J.D. Fowlkes, D.H. Lowndes: Appl. Phys. Lett. **74**, 2322 (1999)
5 C.H. Crouch, J.E. Carey, J.M. Warrender, M.J. Aziz, E. Mazur: Appl. Phys. Lett. **84**, 1850 (2004)
6 R. Younkin. J.E. Carey, E. Mazur, J.A. Levinson, C.M. Friend: J. Appl. Phys. **93**, 2626 (2003)
7 J.E. Carey, C.H. Crouch, M. Shen, M.A. Sheehy, E. Mazur: unpublished results
8 The laser beam has a Gaussian spatial profile; the fluence reported here is the average fluence determined over the entire laser spot, and the peak fluence (in the center of the spot) is twice the average fluence
9 The average number of laser pulses used to structure a sample is defined as $\langle N \rangle = df/s$, where $d =$ the FWHM of the Gaussian beam profile, $f =$ the frequency of the laser pulse train, and $s =$ the scan speed. The natural frequency of the laser pulse train is 1 kHz, but we can reduce the frequency to 150 Hz or less using a fast mechanical shutter
10 Z.R. Zanatta, I. Chambouleyron: Phys. Rev. B **53**, 3833 (1996)
11 www.genplot.com
12 The RBS spectra may be affected slightly by the changing morphology of the surface, as the surface area of the samples changes as processing conditions change. However, the microstructures made with 2, 3, and 5 laser pulses are similar in size and shape, as are the microstructures made with 3, 4, and 5 kJ/m^2, so the sulfur concentrations for those samples can be confidently compared. As the shape of the microstructures is unchanged by annealing, the concentrations before and after annealing can also be compared with confidence

13 E. Janzen, R. Stedman, G. Grossmann, H.G. Grimmeiss: Phys. Rev. B **29**, 1907 (1984)
14 W. Fahrner, A. Goetzberger: Appl. Phys. Lett. **21**, 329 (1972)
15 J.I. Pankove: *Optical Processes In Semiconductors* (New York: Dover Publications, Inc. 1971) p. 9
16 The diffusion length of S in c-Si in 30 minutes at 775 K was estimated to be 25 nm by extrapolation from data In: S.M. Sze: *Physics of Semiconductor Devices*, 2nd ed. (New York: Wiley & Sons 1981) p. 68, In microcrystalline or amorphous silicon, the diffusion length may be somewhat different but is unlikely to increase more than threefold
17 Annealing temperatures that completely eliminate the below-band gap absorptance are much lower than the temperatures at which significant grain growth would be expected in microcrystalline or polycrystalline silicon. See S. Roorda, S. Saito, W.C. Sinke: Mat. Res. Soc. Symp. Proc. **100**, 417 (1988)
18 R. Wilson: J. Appl. Phys. **53**, 3490 (1984)
19 P. Keblinski, S.R. Phillpot, D. Wolf, H. Gleiter: Phys. Lett. A **226**, 205 (1997)
20 F.A. Trumbore: Bell System Tech. J. **39**, 205 (1960)
21 V.I. Emel'yanov, D.V. Babak: Appl. Phys. A **74**, 797 (2002)
22 D. von der Linde, K. Sokolowski-Tinten, J. Bialkowski: Appl. Surf. Sci. **109/110**, 1 (1997)
23 P.G. Carey, T.W. Sigmon: Appl. Surf. Sci. **43**, 325 (1989)
24 R. Reitano, P.M. Smith, M.J. Aziz: J. Appl. Phys. **76**, 1518 (1994)